Age Variation of Wood Anatomical Characteristics in *Larix cajanderi* Tree

Nadezhda I. Blokhina, Olesya V. Bondarenko, and Sergey V. Osipov

Abstract

The paper is the first results of the study of age variation of wood anatomy in *Larix cajanderi* Mayr (Pinaceae). The anatomical study was made from one *L. cajanderi* tree grown in the optimal habitat for *L. cajanderi* within areal of this species. Age variability of anatomical characteristics in the direction from pith to bark and along the height of stem is described in detail. Mature wood in *L. cajanderi* is formed in the base of stem and at breast height in the growth rings numbers 31~40 inclusively, and in the middle of stem in the growth rings numbers 41~50 inclusively. Characteristic features of mature stem wood were not found near the top of tree. Maximal parameters of anatomical characters usually occur in the base of stem. Age variation of wood anatomical characteristics in *L. cajanderi* tree was obtained for the first time.

Key words: *Larix cajanderi*, Pinaceae, wood anatomy, age variability.

Introduction

Larch is one of the main forest forming conifers of the Russian Far East (RFE). However, there is no consensus on number of the *Larix* Mill. species naturally growing in the RFE. For instance, the species *L. cajanderi* Mayr is not a universally recognized taxon and is the subject to be discussed among the specialists. Sukachev (1924) did not recognize *L. cajanderi* as a species taxon and did not even mention it in the work in systematics, phylogeny and historical development of the larches. Sukachev (1924) considered the Dahurian larch, *L. dahurica* Turcz. (= *L. gmelinii* Litv.), in its broadest sense and believed the growing of this larch within the territory of East Siberia (Russia) and adjacent regions of Mongolia and China. According to Ostenfeld and Syrach-Larsen (1930), *L. cajanderi* is synonymous with *L. gmelini* (Rupr.) Gord., which again is the same as *L. dahurica* Turcz. Farjon (1990) recognizes *L. cajanderi* as one of the synonyms of *L. gmelinii* (Rupr.) Kuzen. Fu *et al*. (1999) did not mention *L. cajanderi* in Flora of China; according to those authors, *L. gmelinii* (Rupr.) Kuzen. is spread in Northern China, Korea, Mongolia and East Russia.

Komarov (1934), Dylis (1961), Pozdnjakov (1975) and some other authors considered *L. cajanderi* as the east geographic race or eastern subspecies of *L. gmelinii* (Rupr.) Rupr. – *L. gmelinii* ssp. *cajanderi* (= *L. dahurica* Turcz. ex Trautv. ssp. *cajanderi*) alongside with the west geographic race or western subspecies – *L. gmelinii* ssp. *gmelinii* (= *L. dahurica* ssp. *dahurica*).

According to Kolesnikov (1946), Bobrov (1972, 1978), Cherepanov (1981, 1995), Abaimov and Koropachinskii (1984), Koropachinskii (1989), Nedoluzhko (1995), Muratova (1995, 2004), Muratova and Prokhortchuk (1999), and some others, *L. cajanderi* is an independent species taxon, and we also follow their opinion. However, Milyutin (2003) believes that to date there are no conclusive proofs yet confirming *L. cajanderi* specific status because this larch is not studied enough and *L. gmelinii* as well.

Although, the variation of morphological characteristics of vegetative and generative organs in *L. cajanderi*, in comparison with those of *L. gmelinii*, has been studied by Abaimov and Koropachinskii (1984), Barchenkov and Milyutin (2008), Barchenkov *et al*. (2007) and some others. The karyological investigation of *L. cajanderi* was made by Muratova (1995, 2004), Muratova and Prokhortchuk (1999). *L. cajanderi* differs from *L. gmelinii* in the number of nucleolar regions and their localizations, and the results of the karyosystematic study may be an evidence of the independent specific status of *L. cajanderi* (Muratova and Prokhortchuk 1999). Investigation of genetic variation of allozyme loci in *L. cajanderi* was made by Semerikov *et al*. (1999), Semerikov (2007). Allozymes reveal that the population of *Larix* species defined as *L. cajanderi* appears to be genetically close to both *L. gmelinii* and to *L. olgensis* A. Henry suggesting the origin through introgressive hybridization between these two species (Semerikov *et al*. 1999; Semerikov 2007). However, characteristic features of mature cones (flat, marginally jagged and nonpubescent cone scales) of *L. cajanderi* are close to those of *L. gmelinii*, but other traits (large cones, numerous and sometimes convex or marginally recurved cone scales) resemble more closely those found in either *L. olgensis* or *L. kaempferi* (Lamb.) Sarg. (Semerikov *et al*. 1999). The enzymes of seed endosperms and vegetative buds of *L. cajanderi* were studied by Oreshkova (2008). Vasyutkina *et al*. (2007) investigated *L. cajanderi* population using randomly amplified polymorphic DNA (RAPD) markers. Morphological and anatomical parameters of *L. cajanderi* needles were published by Osipov and Burundukova (2005). Ben'kova and Ben'kova (2006) investigated the climatic factors affecting the variation of radial increment in trees of *L. cajanderi* in comparison with those of *L. gmelinii.* Takahashi *et al*. (2001) studied climatic factors affecting the growth of *L. cajanderi* in the Kamchatka Peninsula.

However, there is no description of the wood anatomy of *L. cajanderi.* Budkevich (1956, 1961) and Greguss (1955, 1963) described the wood anatomy of *L. gmelinii*

considering that species in its broadest sense, i.e. comprising *L. cajanderi*. Greguss described the Dahurian larch as *L. gmelinii* Litv. (Greguss 1955) or *L. gmelinii* (Rupr.) Litv. (Greguss 1963), and Budkevich (1956, 1961) – *L. dahurica* Turcz. Several anatomical characters of the *L. gmelinii* wood also were given in the works "Atlas of wood and fibers for paper" (1992) and "Wood of conifers" (Chavchavadze 1979). Ben'kova and Schweingruber (2004) published three microphotographs of *L. cajanderi* wood anatomical structure; however, they did not give any description of the wood anatomy.

The aim of our study is an attempt to contribute to the description of the wood anatomy of *L. cajanderi*, to the examination of age variability of anatomical characteristics in the direction from pith to bark and along the height of stem, and to the determination of the time of the formation of mature wood which features are important in systematics and diagnostic.

Materials and Methods

The distribution area of the Cajander larch, *L. cajanderi*, is spread to the eastward of the Lena River (Figure 1). *L. cajanderi* grows in the Aldan River basin and further to the north-east, in the basins of rivers Yana, Indigirka, Kolyma, Anadyr and Penzhina, under the conditions of extremely severe climate and very cold soils characteristic of the north-east of RFE. The most of north-east Russia is occupied by vast uplands, and *L. cajanderi* is the only forest forming species within that territory. The larch composes poor productive open woodlands dominated in the landscapes of montane slopes. Besides, *L. cajanderi* occurs in the central Kamchatka Peninsula and partly along the coast of Sea of Okhotsk spreading to the southward up to the Amur River basin. This species of *Larix* also was found in Belichii Island (Shantarskie Islands). Further, *L. cajanderi* is distributed to the south-west of Udskaya Inlet occupying the Aldan-Zeya watershed and Zeya River basin spreading up to the state boundary of Russia (Bobrov 1972, 1978; Abaimov and Koropachinskii 1984; Koropachinskii 1989).

The materials for our study were collected in the montane taiga belt of the Bureya River basin (51° 41' N 134° 18' E 600 m a.s.l., the Amur River basin, RFE) (Figure 1) in 2006 in course of collaborative field trip of the Pacific Institute of Geography FEB RAS and the Far East State University (Vladivostok). The *L. cajanderi* model tree was selected on a river terrace in a larch forest. Height of the terrace is 1 m above river level. It consists of alluvial deposits and does not include permafrost. The vertical structure of the larch forest community consists of tree (*L. cajanderi*), tall scrub (*Duschekia fruticosa* (Rupr.) Pouzar), small scrub (*Ledum hypoleucum* Kom.) and mosses (*Sphagnum girgensohnii* Russ. and *Hylocomium splendens* (Hedw.) B.S.G.) layers. Tree crown density is 70%, tree average height is 24 m, and average diameter is 20 cm. The model tree is characterized with 23.6 m height and 25 cm diameter at breast height. The model tree is healthy and typical for the tree layer of the forest community. Habitat of the community is one of the best (optimal) for *Larix cajanderi* growth in the montane taiga belt of a region.

Figure 1. Distribution area of *Larix cajanderi* and related species *L. gmelinii* (follow Abaimov, Koropachinskii 1984; Bobrov 1972, 1973; Koropachinskii 1989)

The model tree was sawed down. A total of 4 sample disks (1.5~2.0 cm thickness each) were made from the trunk: in the base of tree (32 cm in diameter, 141 growth rings), at the level of 1.3 m above the ground, i.e. at breast height (25 cm in diameter, 138 growth rings), in the middle of tree (in a middle between previous and next disks, i.e. at the level 12.0 m above the ground (17 cm in diameter, 117 growth rings), and 1 m from the top of tree (2.5 cm in diameter, 27 growth rings). From each disk, the triangular sample segment was made from the east side of stem, in total 4 segments. Each segment comprised the pith and all growth rings along the radius of stem up to the bark was split in the blocks in the direction from pith to bark (along the radius of stem) after each ten growth rings; thus, the every block comprised 10 growth rings. Thin transparent sections in mutually perpendicular planes (cross, radial and tangential) were made from the blocks. We used standard technique of preliminary treatment of the wood and preparing thin sections for microscopic investigation given in the works by Yatsenko-Khmelevskii (1954).

The cross and radial sections were made through the pith and comprised all growth rings along the radius of stem. The tangential sections were made in the every growth ring from the ring no. 1 to the ring no. 10 inclusively and further

in the every tenth growth ring, i.e. in the growth rings nos. 20, 30, 40, etc. In total, 1279 thin transparent sections were prepared and microscopically studied. The wood anatomy was described in terms of IAWA List of Microscopic Features for Softwood Identification (IAWA Committee 2004).

Age variability of anatomical characteristics in the direction from pith to bark was studied in the each wood sample disk taken along the height of tree. The cross and radial sections were studied in the every growth ring. The tangential sections were studied in the every growth ring from the ring no. 1 to the ring no. 10 inclusively and further in the every tenth growth ring. Comparative analysis of all the four disks was made to describe the age variability of anatomical characteristics along the height of tree.

Results and Discussion

Age Variability of Anatomical Characteristics along the Radius of Stem (in the direction from pith to bark)

The age variability of anatomical characteristics in *L. cajanderi* along the radius of stem (in the direction from pith to bark) is described in detail at the level of 1.3 m above the ground, i.e. at breast height.

Growth rings are 0.05~3.07 mm, usually 0.5~1.0 mm, wide. Generally, the growth rings become narrower with the age of tree. The age variation of the width of growth rings is given in Figure 2. Growth ring boundaries are distinct (PL. I, Figure 1~6). The transition between early- and latewood is gradual in the growth ring no. 1 (PL. I, Figure 1); the transition becomes marked beginning from the growth ring no. 3 (PL. I, Figure 2), and abrupt from the growth ring no. 5 (PL. I, Figure 3, 4, 6). The latewood occupies 1/6~1/4 of growth ring width in the wide rings, and 1/3~1/2 of the width in narrow rings (PL. I, Figure 3, 4, 6).

In cross section, the outlines of tracheids change with the age of tree. In the growth ring no. 1, both early- and latewood tracheids are rounded-square and practically indistinguishable by their outlines (latewood tracheids are only slightly flattened in radial direction). Beginning from the growth ring no. 2, the earlywood tracheids become more elongated in radial direction, and the latewood tracheids become more flattened. The tracheid diameters and wall thickness change simultaneously. The radial diameter increases from 12~22 μm (growth ring no. 1) up to 34~60 μm (growth ring no. 5) in earlywood tracheids and decreases from 8~20 μm (growth ring no. 1) up to 4~12 μm (growth ring no. 3) in latewood tracheids; further, the radial diameter of tracheids practically does not change neither in early- no in latewood. The tangential diameter changes from 12~20 μm up to 13~31 μm in earlywood tracheids and from 4~12 μm up to 8~17 μm in latewood tracheids. The tracheid wall thickness is 3~4 μm in the growth ring no. 1, beginning from the growth ring no. 2 the wall thickness becomes 2.0~3.5 μm in earlywood tracheids and 4.0~5.5 μm in latewood tracheids; further, the tracheid wall thickness practically does not change neither in early- no in latewood.

In earlywood, tracheid pitting in the radial walls is rear in the first two or three tracheids near the pith. The tracheid pitting is only uniseriate from the growth ring no. 1 to the ring no. 4 inclusively (PL. I, Figure 8, 9; PL. II, Figure 1). The biseriate tracheid pitting appears beginning from the growth ring no. 5. Primarily, the biseriate pitting is rare: one to three pairs opposite pits occur along the length of the tracheid wall. Biseriate pitting becomes abundant beginning from the growth ring no. 15, and dominant from the growth ring no. 33 (PL. I, Figure 11; PL. II, Figure 2, 4).

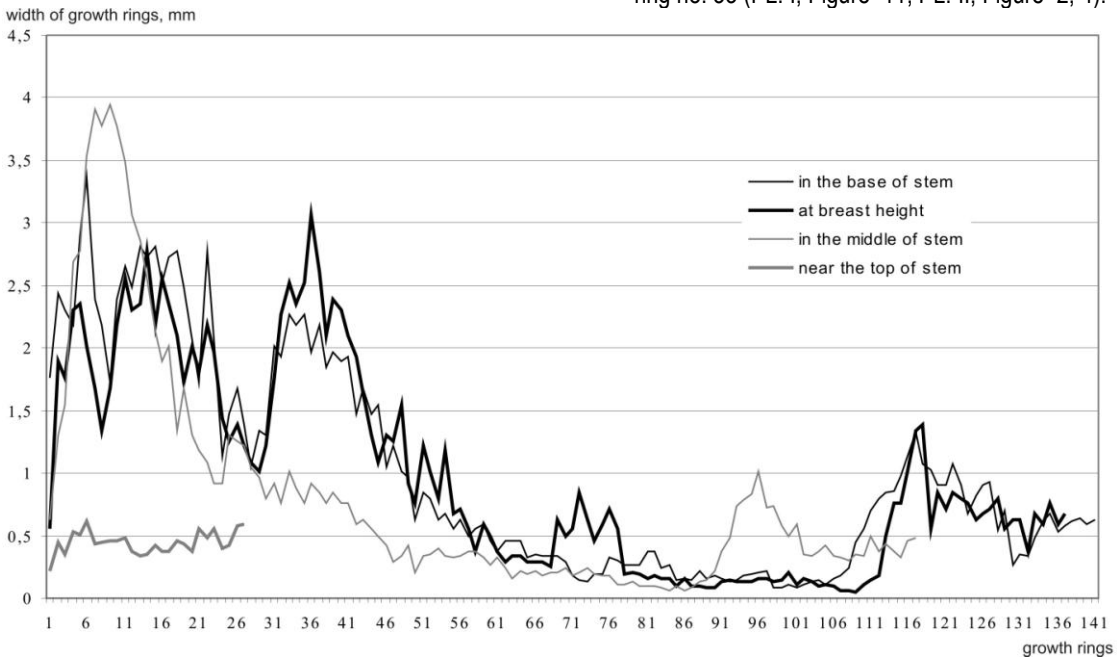

Figure 2. Age variation of the width of growth rings in *Larix cajanderi* along the height of stem.

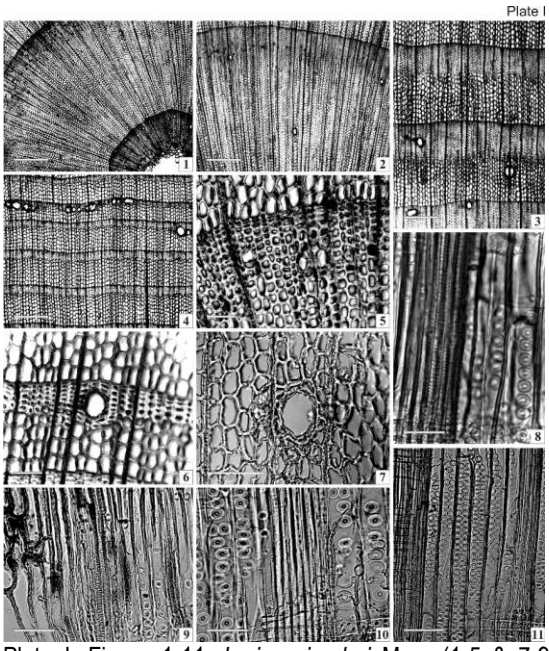

Plate I, Figure 1-11. *Larix cajanderi* Mayr (1-5 & 7-9: sections at the level of 1.3 m above the ground. – 6 & 10, 11: sections in the base of tree). – 1: growth rings nos. 1 & 2, gradual early/latewood transition, axial resin canals normal, axial parenchyma diffuse and abundant. – 2: growth ring no. 4, marked early/latewood transition, axial resin canals normal, axial parenchyma diffuse and scarce. – 3: growth rings nos. 41 & 42, abrupt early/latewood transition, axial resin canals normal, axial parenchyma very scarce and marginal consisting of separate cells on the growth ring boundary. – 4: growth rings nos. 101-105, abrupt early/latewood transition, axial resin canals both normal and traumatic. – 5: growth ring no. 1, growth ring boundary, normal axial resin canals in latewood. – 6: growth ring no. 71, abrupt early/latewood transition, normal axial resin canal in latewood. – 7: growth ring no. 41, normal axial resin canal in earlywood. – 8: growth ring no. 1, helical thickenings in longitudinal tracheids in latewood. – 9: growth ring no. 1, cells of pith, spiral tracheids in primary xylem, pitted tracheids in secondary xylem, tracheid pitting uniseriate, pits circular. – 10: growth ring no. 99, spiral grooves in longitudinal tracheids in latewood. – 11: growth ring no. 49, uniseriate and biseriate pitting in radial tracheid walls in earlywood. – Scale bars: 500 μm in Figure 1-4; 100 μm in Figure 5-7 & 11; 50 μm in Figure8-10.

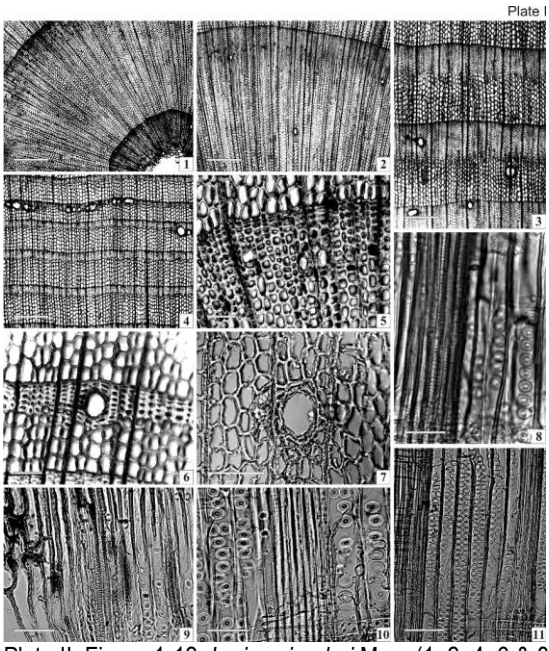

Plate II, Figure 1-12. *Larix cajanderi* Mayr (1, 2, 4, 6 & 8-11: sections at the level of 1.3 m above the ground. – 5: section in the middle of tree. – 3, 7 & 12: sections in the base of tree). – 1: growth ring no. 1, uniseriate pitting in radial tracheid walls in earlywood. – 2: growth ring no. 75, mostly biseriate pitting in radial tracheid walls in earlywood, crassulae between biseriate opposite pits. – 3: growth ring no. 10, tracheid pitting in radial walls in latewood tracheids. – 4: growth ring no. 110, crassulae between both uniseriate and biseriate pits. – 5: growth ring no. 8, tracheid pitting in tangential walls in earlywood. – 6: growth ring no. 2, ray composed of parenchyma cells, a single ray tracheid cell located in the lower margin of ray. – 7: growth ring no. 5, cross-field pitting. – 8: growth ring no. 45, ray tracheids in two marginal cell rows, ray parenchyma cells with pitted horizontal walls and nodular end walls. – 9: growth ring no. 108, ray tracheids in one marginal cell row and fore cell rows in the interior of ray. – 10: growth ring no. 68, ray tracheids in one marginal cell row, maximal number (eight) of cross-field pits. – 11: SEM, growth ring no. 37, cross-field pitting, six and seven pits per cross-field. – 12: SEM, growth ring no. 37, cross-field pit of piceoid type. – Scale bars: 50 μm in Figure 1-9 & 11, 12; 4 μm in Figure 10.

The uniseriate bordered pits are circular and elliptic; the elliptic pits develop beginning from the growth ring no. 3. The number of elliptic pits increases with the age of tree, and circular pits gradually become more characteristic of the latewood tracheids. In the tracheid walls, elliptic pits are in closer arrangement than circular pits. The diameter of uniseriate circular pits increases from 8~10(14) μm (growth rings no. 1) up to 16~29 μm (growth ring no. 33). The dimension of uniseriate elliptic pits increases from 12~16×14~20 μm (growth ring no. 3) up to 18~22×20~28(29) μm (growth ring no. 35). The pit apertures

are included, 8~10 μm in size, circular or elliptic depending on the pit outlines.

The biseriate bordered pits are circular and elliptic; the elliptic pits develop beginning from the growth ring no. 15; however, beginning from the growth ring no. 33, the biseriate circular pits are more common. The diameter of biseriate circular pits increases from 16~18 μm (growth rings nos. 5) up to16~26(28) μm (growth ring no. 45). The dimension of biseriate elliptic pits increases from 14~16×16~20 μm (growth ring no. 15) up to 16~18×18~22 μm (growth ring no. 42). The pit apertures are included, 8~10 μm in size, circular or elliptic depending on the pit outlines. The age variability of pit sizes is given in Tables 1 and 2.

In latewood, tracheid pitting in the radial walls is uniseriate; pits are circular, 8~12 μm in diameter; the largest pits occur in the first latewood tracheids. The pits are widely scattered along the length of the tracheid walls and lacking in the very last latewood tracheids. The pit apertures are included, circular, 5~7 μm in diameter (PL. II, Figure 3).

Crassulae are present in the earlywood tracheids and develop beginning from the growth ring no. 3. The crassulae occur between uniseriate pits and between biseriate pits (predominantly) both circular and elliptic (PL. II, Figure 4).

Table 1. Age variation of *Larix cajanderi* anatomical characters along the radius and height of stem (growth rings nos. 1~10).

Height of stem	Number of consecutive growth rings from pith to bark (along the radius of stem)									
	1	2	3	4	5	6	7	8	9	10
Diameter of uniseriate circular pits (μm)										
Base	8~10(14)	14~18	16~18	16~20	16~20	16~22	16~22	16~22	16~24	16~24
1.3 m	8~10(14)	14~18	16~18	16~20	16~20	16~20	16~20	16~20	16~20	16~24
Middle	8~10(14)	14~18	16~18	16~18	16~20	16~20	16~20	16~20	16~20	16~24
Top	8~10(12)	12~16	14~16	14~16	14~18	14~18	14~18	14~18	16~20	16~20
Dimension of uniseriate elliptic pits (μm)										
Base	—	—	14~16×18~22	14~16×18~22	14~16×18~22	14~16×18~22	14~16×18~22	14~16×18~22	14~16×22~24	16~20×18~24
1.3 m	—	—	12~16×14~20	14~16×18~20	14~16×18~20	14~16×18~20	14~16×18~24	14~16×18~24	14~16×18~24	16~20×18~24
Middle	—	—	12~16×14~18	12~14×16~18	12~16×18~20	12~16×18~20	12~16×18~20	12~16×18~20	12~16×18~20	12~16×18~20
Top	—	—	—	10~12×12~14	12~16×16~20	12~16×16~20	14~18×16~20	14~18×16~20	14~18×16~20	14~18×16~20
Diameter of biseriate circular pits (μm)										
Base	—	—	—	—	—	—	—	—	16~18	16~20
1.3 m	—	—	—	—	16~18	16~20	16~20	16~20	16~20	16~24
Middle	—	—	—	—	—	—	16~18	16~18	16~18	16~18
Top	—	—	—	—	—	—	—	—	—	—
Dimension of biseriate elliptic pits (μm)										
Base	—	—	—	—	—	—	—	—	—	—
1.3 m	—	—	—	—	—	—	—	—	—	—
Middle	—	—	—	—	—	—	—	—	—	—
Top	—	—	—	—	—	—	—	—	—	—
Number of pits per cross-field										
Base	1~4(6)	1~6	1~6	1~6	1~6	1~6	1~6	1~6	1~6	1~6
1.3 m	1~4(5)	1~4(6)	1~6	1~6	1~6	1~6	1~6	1~6	1~6	1~6
Middle	1~3	1~4(5)	1~4(5)	1~4(5)	1~4(6)	1~4(6)	1~6	1~6(7)	1~6(7)	1~6(7)
Top	1~3	1~4(6)	1~4(6)	1~4(6)	1~6	1~6	1~6	1~6	1~6	1~6
Height of uniseriate rays (in number of cells)										
Base	1~16	1~18	1~18	1~18	1~18	1~18	1~18	1~18	1~22	1~22
1.3 m	1~18	1~19	1~19	1~20	1~20	1~20	1~20	1~20	1~20	1~21
Middle	1~15	1~15	1~16	1~16	1~18	1~18	1~21	1~21	1~21	1~22
Top	1~12	1~17	1~17	1~18	1~18	1~18	1~18	1~18	1~18	1~19
Biseriate regions in uniseriate rays (in number of layers)										
Base	1	1	1	1	1	1	1	1	1	1~3
1.3 m	—	—	2	—	—	2~3	—	—	—	2~3
Middle	—	—	—	—		—	1~6	1~3	1~3	1~3
Top	—	—	—	—	1	—	—	—	—	—
Fusiform rays										
Base	—	biseriate	biseriate	biseriate	biseriate	biseriate	biseriate	biseriate	biseriate	biseriate
1.3 m	—	biseriate	biseriate	biseriate	biseriate	biseriate	biseriate	biseriate	biseriate	biseriate
Middle	—	biseriate	biseriate	biseriate	biseriate	biseriate	biseriate	biseriate	biseriate	biseriate
Top	—	biseriate	biseriate	biseriate	biseriate	biseriate	biseriate	biseriate	biseriate	biseriate
Uniseriate extensions in fusiform rays (in number of cells)										
Base	—	1~-3×3~5	1~3×3~5	1~3×3~5	1~3×3~5	1~3×3~5	1~3×3~5	1~3×3~5	2~8×4~12	2~7×4~12
1.3 m	—	1~2×1~4	1~2×2~4	2~3×2~9	1~4×3~10	1~4×3~10	1~4×3~10	1~4×3~10	1~4×3~10	1~4×3~10
Middle	—	2~4×3~6	2~4×3~6	2~4×3~6	2~4×3~6	2~4×3~6	2~4×3~6	2~4×3~6	2~4×3~7	1~8×6~11
Top	—	1~2×2~5	1~2×2~5	1~2×2~5	1~2×2~5	1~2×2~5	1~2×2~5	1~2×2~5	2~3×3~6	2~3×3~6

Tracheid pitting in the tangential walls develops beginning from the growth ring no. 1; pits are circular, 3~5 μm in diameter. In earlywood, pitting in the tangential tracheid walls is abundant, both uniseriate and biseriate (PL. II, Figure 5). The pits are widely scattered along the length of the tracheid wall. In latewood, pitting is rear, uniseriate and lacking in the tracheids near the growth ring boundary.

Helical thickenings occur in latewood in the growth rings nos. 1~4 inclusively (PL. I, Figure 8); further, in some growth rings there are spiral grooves (PL. I, Figure 10).Axial parenchyma is diffuse in the growth ring no. 1 and rather abundant both in latewood and in earlywood. The quantity of axial parenchyma reduces, especially in earlywood, beginning from the growth ring no. 2 (PL. I, Figure 1, 5). The axial parenchyma becomes sparse and marginal consisting of single cells on the growth ring boundaries beginning from the growth ring no. 10 (PL. I, Figure 3, 4, 6). In radial section, the strand of axial parenchyma includes 3~4 cells of 7~9 μm wide and 45~70 μm long. The axial parenchyma cells often contain resinous inclusions. The transverse end walls ofaxial parenchyma cells are smooth and slightly thickened, and the radial walls are pitted with numerous small simple pits in separate arrangement.

The height of uniseriate rays increases from 1~18 cells (growth ring no. 1) up to 1~29 cells. The rays of maximal height appear in the growth rings nos. 31~40 inclusively. The age variability of the height of uniseriate rays is given in Tables 1 and 2. In tangential section, the ray parenchyma cells are 16~24 μm high and 8~14 μm wide beginning from the growth ring no. 1. The horizontal walls of ray parenchyma cells are thickened and distinctly pitted, however, large smooth areas occur relatively often in the walls. The end walls of ray parenchyma cells are nodular (PL. II, Figure 8~10). Indentures are present beginning from the growth ring no. 13. The rays become biseriate in part beginning from the growth ring no. 3; the biseriate regions are as long as 2~3 layers.

Rays are composed solely of parenchyma cells in the growth ring no. 1. Separate ray tracheid cells are developed to the end of the growth ring no. 1 and located in one of the ray margins together with ray parenchyma cells (PL. II, Figure 6). Ray tracheids form a marginal cell row along one of the ray margins beginning from the growth ring no. 3 (PL. II, Figure 7). Ray tracheids are arranged in one or two cell rows along the both ray margins beginning from the growth ring no. 4 (PL. III, Figure 1), and arranged in 1~3(4) rows from the growth ring no. 7 (PL. II, Figure 8~10). Ray tracheids located in one or two cell rows in the interior of the ray become beginning from the growth ring no. 13, and arranged in 3~4 rows from the growth ring no. 23 (PL. II, Figure 9). Sometimes the rays may be composed solely of 1~3 rows of ray tracheids (PL. III, Figure 2); such type of rays is present beginning from the growth ring no. 5. Ray tracheids located along the both ray margins are prevalent. Ray tracheids are low, with thin and smooth interior walls and often with sinuous external walls; the radial walls of ray tracheid cells are pitted with bordered circular pits 4.5~6.0 μm in diameter (PL. II, Figure 8~10; Pl. III, Figure 1). Ray tracheid cells become lower and elongated along the ray with the age of tree.

In earlywood, the cross-fields are vertically elongated in radial section within the growth ring no. 1. The cross-fields of square outlines are present beginning from the growth ring no. 2 (PL. II, Figure 7), and horizontally elongated cross-fields occur from the growth ring no. 5. The cross-field pits are piceoid (PL. II, Figure 12), 4~6 μm in diameter. There are 1~4(5) pits per cross-field in the growth ring no. 1 (PL. II, Figure 7); 6 pits per cross-field appear beginning from the growth ring no. 2, and 8 pits (maximum pit numbers) occur from the growth ring no. 16 (PL. II, Figure 10, 11). Pits are arranged in a single horizontal row in case of 2 or 3 pits are present in cross-field, in two horizontal rows in case of 3 to 8 pits, and diffuse in case of 3 to 5 pits. The age variability of pit numbers per cross-field is given in Tables 1 and 2.

Axial resin canals are normal, develop beginning from the growth ring no. 1, and usually occur within transitional zone from early- to latewood or in the latewood. The resin canals are solitary or, occasionally, occur in pairs. In cross section, resin canals are circular or elliptic, radially elongated (PL. I, Figure 1~7). The diameter of axial resin canals increases with the age of tree from 9~18 μm (growth ring no. 1) up to 20~60 μm (beginning from the ring no. 32). The epithelial cells are thick-walled, the number of epithelial cells increases with the age of tree from 5~7 cells (growth ring no. 1) (PL. I, Figure 5) up to 7~12 cells (beginning from the ring no. 32) (PL. I, Figure 6, 7).

Table 2. Age variation of *Larix cajanderi* anatomical characters along the radius and height of stem (from the growth ring no. 11 to the bark).

Height of stem	Number of consecutive growth rings from pith to bark (along the radius of stem)			
	11~20	21~30	31~40	41~50 to bark
	Diameter of uniseriate circular pits (μm)			
Base	16~24	16~26	16~29	16~29
1.3 m	16~24	16~28	16~29	16~29
Middle	16~24	16~24	16~24	16~24(26)
Top	16~20	16~20	—	—
	Dimension of uniseriate elliptic pits (μm)			
Base	16~20×18~24	18~22×20~28(29)	18~22×20~28(29)	18~22×20~28(29)
1.3 m	16~20×18~24	18~22×20~28	18~22×20~28(29)	18~22×20~28
Middle	12~16×18~20	12~16×18~20	12~16×18~20	16~18×20~24
Top	16~18×20~24	16~18×20~24	—	—
	Diameter of biseriate circular pits (μm)			
Base	16~22	16~24	16~26(28)	16~26(28)
1.3 m	16~24	16~24	16~26	16~26(28)
Middle	16~18	16~20	16~20	16~20
Top	—	14~16(20)	—	—
	Dimension of biseriate elliptic pits (μm)			
Base	16~18×18~22	16~18×18~22	16~20×18~24	16~20×18~24
1.3 m	14~16×16~20	14~18×16~22	14~18×16~22	16~18×18~22
Middle	—	—	—	14~16×16~20
Top	—	—	—	—
	Number of pits per cross-field			
Base	1~6(7)	1~6(8)	1~6(8)	1~6(8)
1.3 m	1~6(8)	1~6(8)	1~6(8)	1~6(8)
Middle	1~6(7)	1~6(7)	1~6(7)	1~6(8)
Top	1~6	1~6	—	—
	Height of uniseriate rays (in number of cells)			
Base	1~28	1~30	1~30	1~30
1.3 m	1~26	1~26	1~29	1~29
Middle	1~22(24)	1~22(24)	1~26	1~26
Top	1~20	1-~20	—	—
	Biseriate regions in uniseriate rays (in number of layers)			
Base	1~3	1~3	1~7(9)	1~5
1.3 m	2~3	2~3	2~3	2~3
Middle	1~3	—	—	—
Top	—	—	—	—
	Fusiform rays			
Base	biseriate bi-triseriate triseriate —	biseriate bi-triseriate triseriate —	biseriate bi-triseriate triseriate —	biseriate bi-triseriate triseriate tri-quadriseriate
1.3 m	biseriate bi-triseriate —	biseriate bi-triseriate —	biseriate bi-triseriate triseriate	biseriate bi-triseriate triseriate
Middle	biseriate — —	biseriate bi-triseriate —	biseriate bi-triseriate —	biseriate bi-triseriate triseriate
Top	biseriate	biseriate	—	—
	Uniseriate extensions in fusiform rays (in number of cells)			
Base	2~10×4~15	2~10×4~15	1~8×5~21	1~8×5~21
1.3 m	4~6×4~14	4~6×4~14	4~11×7~16	4~11×7~16
Middle	1~9×6~11(13)	1~11×6~17	3~13×5~15	3~13×5~15
Top	2~3×3~6	2~3×3~6	—	—

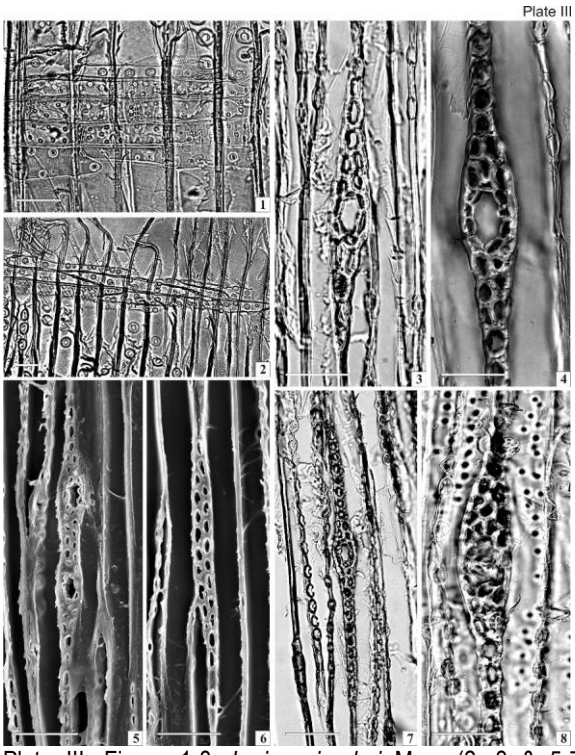

Plate III, Figure 1-8. *Larix cajanderi* Mayr (2, 3 & 5-7: sections at the level of 1.3 m above the ground. – 4 & 8: sections in the base of tree. – 1: section in the top of tree). – 1: growth ring no. 25, ray tracheids in a single row along the both ray margins. – 2: growth ring no. 50, ray composed of ray tracheids. – 3: growth ring no. 2, biseriate fusiform ray, radial resin canal normal, uniseriate extensions at both ends of the ray short and equal. – 4: growth ring no. 70, bi- triseriate fusiform ray, radial resin canal normal. – 5: SEM, growth ring no. 40, biseriate fusiform ray, two radial resin canals. – 6: SEM, growth ring no. 50, ray biseriate in part. – 7: growth ring no. 100, biseriate fusiform ray, radial resin canal normal, uniseriate extensions at both ends of the ray long and equal. – 8: growth ring no. 80, tri-quadriseriate fusiform ray, radial resin canal normal. – Scale bars: 50 μm in Figure 1-6, 8; 100 μm in Figure 7.

Radial resin canals are normal and occur in the rays beginning from the growth ring no. 2 (PL. III, Figure 3). In tangential section, resin canals are circular or elliptic elongated along the length of the ray, 9~35 μm in dimension. The epithelial cells are thick-walled, and the number of epithelial cells increases with the age of tree from 4~7 cells (growth ring no. 2) (PL. III, Figure 3) up to 6~9 cells (growth rings nos. 11~20 inclusively) (PL. III, Figure 4, 7). The width of fusiform rays increases with the age of tree and is given in Table 1 and 2. Exclusively biseriate fusiform rays occur in the growth rings nos. 2~10 inclusively. Bi-triseriate fusiform rays (PL. III, Figure 4) appear in the growth rings nos. 11~20 inclusively. Triseriate rays appear in the growth rings nos. 31~40 inclusively. The uniseriate extensions in fusiform rays are equal and short (1~4 cells) in the growth ring no. 2 (PL. III, Figure 3); the equal long uniseriate extensions of 10~16 cells appear in the growth rings nos. 31~40 inclusively (PL. III, Figure 7). The unequal uniseriate extensions of 4~14 cells appear in the growth rings nos. 11~20 inclusively, and the greatly unequal extensions of 5~21 cells in the growth rings nos. 31~40 inclusively. The age variability of uniseriate extensions is given in Tables 1 and 2.

Age Variability of Anatomical Characteristics along the Height of Stem

The age variability of anatomical characteristics in *L. cajanderi* along the height of tree is given in Table 3. Comparative analysis of all the four disks showed the following peculiarities:

In the base of stem, pits of maximal size in the radial tracheid walls, uniseriate rays of maximal height, and bi-triseriate and triseriate fusiform rays appear earlier than at the level of 1.3 m above the ground (at breast height). For instance, the uniseriate circular pits 29 μm in diameter appear beginning from the growth ring no. 31, whereas at breast height they develop from the ring no. 33. The uniseriate elliptic pits 18~22×20~28(29) μm in dimension appear beginning from the growth ring no. 29, and at breast height from the ring no. 35. The biseriate circular pits 16~26(28) μm in diameter appear beginning from the growth ring no. 31, whereas at breast height they develop from the ring no. 45. The biseriate elliptic pits 16~20×18~24 μm in dimension appear beginning from the growth ring no. 34, and at breast height from the ring no. 42. The uniseriate rays of 30 cells high appear in the growth rings nos. 21~30 inclusively. Bi-triseriate and triseriate fusiform rays appear in the growth rings nos. 11~20 inclusively. Tri-quadriseriate fusiform ray was found in the growth rings nos. 40 and 80 in the base of stem.

In the base of stem, biseriate pits both circular and elliptic in the radial tracheid walls, and maximum pit numbers per cross-field appear considerably latter than at breast height. For example, the biseriate circular pits develop beginning from the growth ring no. 9, and biseriate elliptic pits from the growth ring no. 14, at breast height they develop beginning from the growth rings nos. 5 and 15 respectively. Eight pits occur in cross-fields beginning from the growth ring no. 23, and at breast height from the growth ring no. 16.

In the middle of stem and near the top of tree all diagnostic characters appear latter than in the base of stem and at breast height, with the exception of biseriate circular pits in the radial tracheid walls. These pits appear in the middle of stem earlier (growth ring no. 7) than in the base of stem (growth ring no. 9), and latter than at breast height (growth ring no. 5).

In the base of stem, anatomical characters usually are of maximal parameters. For instance, pits of maximal size are common in the radial tracheid walls, maximum pit

numbers per cross-fields and maximum rows of ray tracheids located in the interior of the ray occur more frequent, triseriate fusiform rays are prevalent, and tri-quadriseriate fusiform ray was found in the base of stem. In the base of stem, there are also the highest uniseriate rays (up to 30 cells high) with the longest biseriate regions (7~9 cells), fusiform rays have the longest equal and greatly unequal uniseriate extensions, resin canals both axial and radial are enclosed with maximum number of epithelial cells, and the average mean of growth ring width is the greatest (1.0 mm). In the base of stem, ray tracheids located in 7 cell rows along one of the ray margins were found in the ray.

In the middle of stem there are the widest growth rings (3.95 mm wide) and the thickest walls in both early- and latewood tracheids. However, in the middle of stem, in contrast to the base of stem and at breast height, there are lower uniseriate rays, smaller pit sizes in the radial tracheid walls, lesser number of epithelial cells in both axial and radial resin canals, shorter uniseriate extincsions in the fusiform rays, and rare occurrence of triseriate rays (they are not found in every section).

Near the top of tree anatomical characters have minimal parameters: growth rings are 0.22~0.61mm wide, uniseriate rays are not more than 20 cells high, fusiform rays are solely biseriate with very short and equal (1~3(6) cells) uniseriate extensions, and there are not more than 6 pits per cross-field. Near the top of tree ray tracheids are located along the ray margins or in the interior of the ray not more than in one or two rows, and the rays comprised solely of ray tracheids are extremely rear. Near the top, the biseriate elliptic pits are lacking in the radial tracheid walls, and rays biseriate in part are absent.

Comparative analysis of the age variability of anatomical characteristics along the radius and height of stem has shown that generally mature wood in *L. cajanderi* is forming in the base of stem and at breast height in the growth rings nos. 31~40 inclusively, whereas in the middle of stem mature wood is forming in the growth rings nos. 41~50 inclusively. Near the top of tree, anatomical features characteristic the mature stem wood are not forming.

Description of Mature Wood Anatomy

Mature wood anatomy of *L. cajanderi* is described on the basis of anatomical characteristics of mature wood in all the four disks along the height of tree (Table 3).

Growth rings are distinct, 0.05~3.95 mm wide. The earlywood/latewood transition is abrupt. The latewood occupies 1/6~1/4 of growth ring width in the wide rings, and 1/3~1/2 of the width in narrow rings (PL. I, Figure 3, 4, 6). The earlywood tracheids in cross section are thin walled, rectangular, elongated in radial direction, with broad lumina; the latewood tracheids are thick walled, rectangular, strongly flattened in radial direction, with nearly slitlike lumina near the growth ring boundary (PL. I, Figure 6). The earlywood tracheids are 10~36×20~60 μm, and the latewood tracheids are 4~28×8~32 μm in dimensions. The thickness of earlywood tracheid walls is 2~4 μm, and the latewood tracheids 4~10 μm.

Tracheid pitting in the radial walls is abundant in earlywood (PL. I, Figure 11; Pl. II, Figure 2, 4), uniseriate and biseriate opposite (prevalent). The uniseriate bordered pits are circular and elliptic, 16~24(29) μm in diameter or 18~22×20~28(29) μm in dimension respectively. The biseriate bordered pits are circular and elliptic, 16~26(28) μm in diameter or 16~20×18~24 μm in dimension respectively. The pit apertures are included, circular and elliptic depending on the pit outlines, 8~10 μm in size.

In latewood, tracheid pitting in the radial walls is uniseriate, pits are widely scattered along the length of the tracheid wall and lacking in the very last latewood tracheids (PL. II, Figure 3). Pits are bordered, circular, 8~12 μm in diameter; the pit apertures are included, circular, 5~7 μm in diameter.

Tracheid pitting in the tangential walls is abundant in earlywood and rear in latewood lacking in the tracheids near the growth ring boundary. In earlywood, the pitting is both uniseriate and biseriate (PL. II, Figure 5), and in latewood the pitting is uniseriate. Pits are circular, 3~5 μm in diameter, widely scattered along the length of the tracheid wall.

Crassular are present in the earlywood tracheids and occur between uniseriate pits and between biseriate pits (predominantly) both circular and elliptic (PL. II, Figure 4). Helical thickenings are absent; although in several growth rings there are spiral grooves in the latewood tracheids (PL. I, Figure 10).

Axial parenchyma is sparse and marginal consisting of single cells on the growth ring boundaries (PL. I, Figure 3, 4, 6). In radial section, the strand of axial parenchyma includes 3~4 cells of 7~9 μm wide and 45~70 μm long. The transverse end walls of axial parenchyma cells are smooth and slightly thickened, and the radial walls are pitted with numerous small simple pits in separate arrangement. The axial parenchyma cells often contain resinous inclusions.

Rays are 1~30 cells high, uniseriate sometimes biseriate in part, with biseriate regions of 1~3(6~9) layers (PL. III, Figure 6). In tangential section, ray cells are16~24 μm high and 8~14 μm wide. The horizontal walls of ray parenchyma cells are thickened and distinctly pitted, however, large smooth areas occur relatively often in the walls; the end walls are nodular (PL. II, Figure 8~10). Indentures are present. Ray tracheids are low, with thin and smooth interior walls and often with sinuous external walls; the radial walls are pitted with bordered circular pits 4.5~6.0 μm in diameter. Ray tracheids are located in 1~3(4) cell rows along the both ray margins (PL. II, Figure 8~10; Pl. III, Figure 1) or in 1~2(3~4) rows in the interior of the ray (PL. II, Figure 9). In a single ray, ray tracheids are arranged in 7 cell rows along one of the ray margins. Sometimes, rays are composed solely of 1~2(3) rows of ray tracheids (PL. III, Figure 2). The rays containing ray tracheids arranged in cell rows along both ray margins are prevalent.

Table 3. Comparison of anatomical characteristics of *Larix cajanderi* mature wood along the height of stem.

Anatomical characters	Base of stem	Breast height	Middle of stem	Near top of stem
Diameter of sample wood disk, cm	32	25	17	2.5
Number of growth rings	141	138	117	27
Width of growth rings, mm (min-max/mean ± error)	0.08~3.36/1.0 ±0.853	0.05~3.07/0.96±0 .806	0.06~3.95/0.82±0 .923	0.22~0.61/0.45±0 .090
Thickness of tracheid walls, µm:				
in earlywood	3~4	2~3.5	3~4	2~3
in latewood	5~8	4~5.5	6~10	4~6
Dimensions of tracheid lumina, µm:				
in earlywood	24~36×20~56	13~31×34~60	16~40×32~60	10~28×28~40
in latewood	4~28×14~32	4~12×8~17	4~16×14~20	4~12×8~16
Pits in radial tracheid walls:				
uniseriate	+	+	+ +	+ +
circular	+	+	+	+
elliptic	+ +	+ +	+ +	+
biseriate	+ +	+ +	+	+ −
circular	+ +	+ +	+	+
elliptic	+	+	+ −	−
pit diameters, µm -				
in earlywood	16~24(29)	16~24(29)	16~24(26)	16~20(24)
in latewood	12~14	12~14	12~14	12~14
Pit diameters in tangential tracheid walls, µm:	3~5	3~5	3~5	3~5
Uniseriate rays:				
height (in number of cells)	1~30	1~29	1~26	1~20
biseriate regions (in number of layers)	1~7(9)	1~3	1~3(6)	−
Axial resin canals:				
number of epithelial cells	7~12	7~10(12)	8~11	7~9(10)
diameter of canals, µm:	32~60×40~84	36~68×56~92	28~68×32~72	20~40×32~60
Radial resin canals:				
number of epithelial cells	7~10(12)	7~9(10)	7~10(11)	7~9
diameter of canals, µm:	12~24×20~40	16~20×32~40	12~24×28~48	12~20×20~32
fusiform rays -				
biseriate	+	+	+ +	+
bi-triseriate	+	+	+	−
triseriate	+	+	+ −	−
tri-quadriseriate	+ − −	−	−	−
uniseriate extensions in fusiform rays (in number of cells) -				
short	1~14	1~14	1~11	2~3
long	3~20	3~16	3~17	3~6
Ray tracheids (number of cell rows):				
along ray margins	1~4(7)	1~4	1~3	1~2
in the interior of ray	1~4	1~3(4)	1~2(3)	1(2)
individual ray	1~3	1~3	1~2(3)	1~2
Cross-field pitting:				
number of pits per cross-field	1~8	1~6(7~8)	1~6(7~8)	1~4(5~6)
pit diameters, µm	4~6	4~6	4~6	4~6
pits of piceoid type	+	+	+	+

There are 1~6(7~8) pits of the piceoid type per cross-field; pits are 4~6 μm in diameter (PL. II, Figure 10, 11).

Axial resin canals are normal, lined by 7~12 thick-walled epithelial cells. Resin canals are solitary or, occasionally, in pairs, generally located in the transitional zone between early- and latewood or in the latewood (PL. I, Figure 3, 4, 6, 7). In cross section, resin canals are circular or elliptic, radially elongated, 20~68×32~92 μm in dimensions.

Radial resin canals are normal, surrounded by 7~10(12) thick-walled epithelial cells. In tangential section, resin canals are circular or elliptic elongated along the ray, 12~24×20~48 μm in dimensions. Resin canals occur in biseriate (PL. III, Figure 3, 7), bi-triseriate (PL. III, Figure 4), triseriate and, occasionally, in tri-quadriserate fursiform rays (PL. III, Figure 8). Sometimes there are 2~3 radial resin canals in the same ray (PL. III, Figure 5). Uniseriate extensions in the fusiform rays are equal short (1~4 cells) (PL. III, Figure 3) or long (10~16 cells) (PL. III, Figure 7), and also unequal: short extensions consist of 1~5 cells and long extensions consist of 4~14 cells, or sometimes, greatly unequal consisting of 5~21 cells.

Conclusions

The current study of age variability of anatomical characteristics made in the direction from pith to bark and along the height of stem of *L. cajanderi* model tree selected from the optimal habitat for this larch growth in the montane taiga belt of the Amur River basin (RFE) is contributed to the description of the wood anatomy of the species *L. cajanderi*. Wood anatomy of *L. cajanderi* is described for the first time.

The time of the formation of *L. cajanderi* mature wood has been determined. Mature wood in the *L. cajanderi* model tree is forming in the base of stem and at breast height in the growth rings nos. 31~40 inclusively, and in the middle of stem in the growth rings nos. 41~50 inclusively. Features characteristic mature stem wood are not forming near the top of tree.

The wood anatomy of *L. cajanderi* model tree showed characteristics that are lacking in the descriptions of the wood anatomy of *L. gmelinii* given by Budkevich (1956, 1961), Greguss (1955, 1963), Chavchavadze (1979), and in the "Atlas of wood and fibers for paper" (1992). Several anatomical features, such as triseriate, quadriseriate and fiveseriate tracheid pitting in the radial walls, and cross-field pits of taxodioid type were not found in the wood of *L. cajanderi* model tree studied. In *L. cajanderi*, tracheid pitting in the radial walls is uniseriate and biseriate, and cross-field pits are of piceoid type. In *L. cajanderi*, there are up to 8 pits per cross-field, whereas in the anatomical descriptions of *L. gmelinii* we found not more then 6(7) pits per cross-field. Cross-field pits in *L. cajanderi* are smaller (4~6 μm in diameter) than those in *L. gmelinii* (6~7(8) μm in diameter).

Acknowledgement

This work was supported by the Russian Foundation for Basic Research (project no. 08-04-00419), and the Presidium of the Russian Academy of Sciences and the Presidium of the Far East Branch of the Russian Academy of Sciences (project no. 09-I-P15-02).

References

Abaimov, A.P.; I.Y. Koropachinskii. 1984. The Cajander (*Larix cajanderii*) and Gmelin (*L. gmelinii*) Larchs. Nauka, Novosibirsk [in Russian].

Atlas of Wood and Fibers for Paper. 1992. E.S. Chavchavadze (ed.). Izdatel'stvo "Kluch", Moscow [in Russian].

Barchenkov, A.P.; L.I. Milyutin; A.P. Isaev. 2007. The Variability of Seeds in Siberian Larch Species. Lesovedenie 2: 65-69 [in Russian].

Barchenkov, A.P.; L.I. Milyutin. 2008. The Variability of Generative Organs in Gmelin (*L. gmelinii*) and Cajander (*Larix cajanderii*) Larchs of East Siberia. Khvoinye Boreal'noi Zony 25(1-2): 37-43 [in Russian].

Ben'kova, V.E.; F.H. Schweingruber. 2004. Anatomy of Russian Woods (An atlas for the identification of trees, shrubs, dwarf shrubs and woody lianas from Russia). Haupt Verlag, Bern, Stuttgart, Wien.

Ben'kova, V.E.; A.V. Ben'kova. 2006. Specific Features of Wood Structure in Siberian Larch Species. Lesovedenie 4: 28-36 [in Russian].

Bobrov, E.G. 1972. The History and Systematics of the Larches. In: E.G. Bobrov (ed.), Komarov Letters 25: 1-96. Nauka, Leningrad [in Russian].

Bobrov, E.G. 1978. The Forest Formation Conifers of the USSR. Nauka, Leningrad [in Russian].

Budkevich, E.V. 1956. Anatomical Structure of the *Larix* species in Connection with their Systematics. Botanical Zhurnal 41(1): 64-80 [in Russian].

Budkevich, E.V. 1961. The Wood of the Pinaceae. Izdatel'stvo Akad. Nauk SSSR, Moscow, Leningrad [in Russian].

Chavchavadze, E.S. 1979. Wood of Conifers. Nauka, Leningrad [in Russian].

Cherepanov, S.K. 1981. Vascular Plants of the USSR. Nauka, Leningrad.

Cherepanov, S.K. 1995. Vascular Plants of Russia and Adjacent States (within the former USSR). Izdatel'stvo «Mir i Sem'ya», St. Petersburg [in Russian].

Dylis, N.V. 1961. The Larch in East Siberia and Far East. Izdatel'stvo Akad. Nauk SSSR, Moscow [in Russian].

Farjon, A. 1990. Pinaceae: Drawings and Descriptions of the Genera *Abies*, *Cedrus*, *Pseudolarix*, *Keteleeria*, *Nothotsuga*, *Tsuga*, *Cathaya*, *Pseudotsuga*, *Larix* and *Picea*. Regnum Vegetabile. 121. Koeltz Scientific Books, Königstein.

Fu, L.; Li-kuo, Fu; R.R. Mill. 1999. Larix. In: Wu Zheng-yi, P.H. Raven (eds.), Flora of China. V. 4. (Cycadaceae to Fagaceae): 33-37. Science Press, Beijing; Missouri Bot. Gard. Press., St. Lois.

Greguss, P. 1955. Xylotomische Bestimmung der heute Lebenden Gymnospermen. Akad. Kiadó, Budapest.

Greguss, P. 1963. The Key for Identification of Gymnosperm Wood by Microscopic Features. Izdatel'stvo Lomonosov Moscow State Univ., Moscow [in Russian].

IAWA Committee. 2004. IAWA List of Microscopic Features for Softwood Identification. H.G. Richter, D. Grosser, I. Heinz, P.E. Gasson (eds.). IAWA Journal 25(1): 1-70.

Kolesnikov, B.P. 1946. To the Taxonomy and the Historical Development of Larches (section Pauciseriales Patschke). In: V.L. Komarov (ed.), Materials on the History of the Flora and Vegetation of the USSR. II: 321-364. Izdatel'stvo Akad. Nauk SSSR, Moscow, Leningrad [in Russian].

Komarov, V.L. 1934. The Conifers. In: V.L. Komarov (ed.), The Flora of the USSR. I: 130-195. Izdatel'stvo Akad. Nauk SSSR, Moscow, Leningrad [in Russian].

Koropachinskii, I.Yu. 1989. The Family Pinaceae. In: S.S. Kharkevich (ed.), Vascular Plants of the Soviet Far East. IV: 9-20. Nauka, Leningrad [in Russian].

Milyutin, L.I. 2003. Biodiversity of Russian Larches. Khvoinye Boreal'noi Zony 1: 6-9 [in Russian].

Muratova, E.N. 1995. The Peculiarities of the Cajander Larch (*Larix cajanderi* Mayr) Karyotype. In: V.L. Cherepnin (ed.), Botanical Researches in Siberia. 3: 10-22. Izdatelo'stvo Siberia State Technological Univ., Krasnojarsk [in Russian].

Muratova, E.N. 2004. The Systematic Relationships in the Genus *Larix* on the Basis of Karyology and DNA Analysis Data. Vestnik Tomsk State Univ. 10: 59-63 [in Russian].

Muratova, E.N.; E.N. Prokhortchuk. 1999. Karyosystematic Studies of Far Eastern Conifers. In: Yu.I. Man'ko (ed.), Forests and Forest Formation Process in the Far East: Proceed. Intern. Conf. Devoted to the 90th Anniversary of B.P. Kolesnikov: 203-204. Izdatel'stvo Institute of Biogoly and Soil Science FEB RAS, Vladivostok [in Russian].

Nedoluzhko, V.A. 1995. Synopsis of Aboriflora of the Russian Far East. Dal'nauka, Vladivostok [in Russian].

Oreshkova, N.V. 2008. Allozyme Polymorphism of the Enzymes in Siberian Larch (*Larix sibirica* Ledeb.) and Cajander Larch (*Larix cajanderi* Mayr). Conifers of Boreal Zone 25(1-2): 160-168 [in Russian].

Osipov, S.; O. Burundukova. 2005. Characteristics of Cajander Larch (*Larix cajanderi* Mayr) on Dredging Waste Dumps in the Amur Region. Russian Journal Ecology 36(4): 234-238.

Ostenfeld, C.H.; C. Syrach-Larsen. 1930. The Species of the Genus *Larix* and their Geographical Distribution. Det. Kongelige Danske Videnskabemes Selskabs Biologiske Meddelelser. 9(2): 1-107.

Pozdnjakov, L.K. 1975. The Daur Larch (*Larix dahurica*). Nauka, Moscow [in Russian].

Semerikov, V.L.; L.F. Semerikov; M. Lascoux. 1999. Intra- and Interspecific Allozyme Variability in Eurasian *Larix* Mill. Species. Heredity 82: 193-204.

Semerikov, V.L. 2007. Population Structure and Molecular Systematics of the *Larix* Mill. Species. Abstract of Dr. Sci. Thesis in Biology. Yekaterinburg [in Russian].

Sukachev, V.N. 1924. To the Historical Development of Larches. In: M.E. Tkachenko (ed.), Lesnoe Delo: 12-44. Izdatel'stvo People's Commissariat Agriculture «Novaja Derevnja», Moscow, Leningrad [in Russian].

Takahashi, K.; K. Hommak; T. Shiraiwa; V.P. Vetrova; T. Hara. 2001. Climatic Factors Affecting the Growth of *Larix cajanderi* in the Kamchatka Peninsula, Russia. Eurasian Journal of Forest Research 3: 1-9.

Vasyutkina, E.A.; I.Yu. Adrianova; M.M. Kozyrenko; E.V. Artukova; G.D. Reunova; Yu.N. Zhuravlev. 2007. Genetic Differentiation of Larch Populations from the *Larix olgensis* Range and their Relationships with Larches from Siberia and Russian Far East. Forest Science and Technology 3(2): 132-138.

Yatsenko-Khmelevskii, A.A. 1954. Principals and Methods of Anatomical Investigation of the Wood. Izdatel'stvo Akad. Nauk SSSR, Moscow, Leningrad [in Russian].

Nadezhda I. Blokhina, and Olesya V. Bondarenko
Institute of Biology and Soil Science, Far Eastern Branch, Russian Academy of Sciences,
Prospect Stoletiya 159, Vladivostok 690022, Russia,
Fax. : +7(4232)310-193
E-mail : blokhina@biosoil.ru, laricioxylon@gmail.com

Sergey V. Osipov
Pacific Institute of Geography, Far East Branch, Russian Academy of Sciences,
Radio Str. 7, Vladivostok 690041, Russia,
Fax. : +7(4232)312-159
E-mail : sv-osipov@yandex.ru